Eur. Radiol. (2001) 11: 1470–1482
DOI 10.1007/s003300000751

Jean Garcia
Stefano Bianchi

Diagnostic imaging of tumors of the hand and wrist

Received: 6 June 2000
Revised: 5 October 2000
Accepted: 5 October 2000
Published online: 6 January 2001

J. Garcia (✉) · S. Bianchi
Département de Radiologie,
Division de Radiodiagnostic et Radiologie Interventionnelle,
Hôpital Cantonal Universitaire de Genève,
Rue Micheli-du-Crest 24, 1211 Geneva, Switzerland
E-mail: Jean.F.Garcia@hcuge.ch
Phone: +41-22-372 33 11
Fax: +41-22-372 70 72

Abstract Tumors of the hand and wrist most commonly result from dystrophic lesions and hamartomas. Neoplastic lesions are rare. Imaging modalities are required for their detection and accurate location, careful assessment of the internal structure and borders, evaluation of the relation with surrounding tendons, nerves, and vessels, and are also required for staging. A variety of imaging techniques, including standard radiographs, sonography, CT, and MRI, can be obtained. The aim of this article is to present paradigmatic images of a variety of expansible lesions of the hand and wrist and to describe and compare the diagnostic findings of different imaging techniques.

Keywords Hand · Wrist · Tumors · Sonography · Ultrasound · CT · MRI

Introduction

Expansible lesions of the hand are more frequently dystrophic lesions and hamartomas, rather than true neoplastic diseases, and affect all groups of age without a definite gender preponderance [1]. They are mainly benign lesions that originate from different structures including the skin, subcutaneous fat, synovium, cartilage, and bone, whereas tendon involvement is unusual [1].

Malignant tumors are rare. A variety of imaging techniques, including plain radiographs, US, CT, and MR imaging, can image tumors of the hand and wrist. Plain radiographs must be obtained in all patients since they are inexpensive and panoramic. Ultrasound, if performed by an experienced operator utilizing high-definition probes, can accurately assess the internal structure of the mass and the relation with the adjacent nerves and vessels. Moreover, color Doppler US can assess the internal vascularity. Because of multiplanar capability and excellent tissue contrast, MRI is rapidly substituting CT in the assessment of the extension of the mass, although CT is still the method of choice in evaluating small bone tumors such as osteoid osteoma. Whether a malignant tumor is considered, additional imaging modalities, including MDP Tc99m, chest film, and CT for possible detection of bone or pulmonary metastases, are essential.

Bone tumors

The frequency of bone tumors affecting the hand is low. In Dahlin's series of 4277 primitive bone tumors only 2% were located in the hand or wrist [2]. Murray et al., in a series of 26,800 bone neoplasms, found 44 primary tumors of carpal bone (0.16%) [3]. Distribution of tumor among different bones of the hand was evaluated by Wilner [4] (Tables 1, 2). Furthermore, bone tumors are rare compared with other tumors of the hand. Haber et al., in a series of 2321 tumors of the hand, reported 38 cases affecting the bone (2%) [5]. Other series demon-

Table 1 Distribution of benign bone tumors (%) (From Wilner's data [4])

Type	Carpal bones	Metacarpals	Phalanges
Osteoid osteoma	2	3	5
Osteoblastoma	1	5	3
Osteochondroma		1	< 1
Enchondroma		10	40
Chondroblastoma	< 1	1	1
Hemangioma	None		
Giant cell tumor		1	< 1
Aneurysmal bone cyst	< 1	1	1

Table 2 Distribution of malignant bone tumors (%) (From Wilner's data [4])

Type	Carpal bones	Metacarpals	Phalanges
Osteogenic sarcoma		< 1	< 1
Juxtacortical sarcoma		1	
Chondrosarcoma	2 (whole hand)		
Fibrosarcoma			
Ewing's tumor		< 1	< 1
Post-irradiation SA	2		2
Multiple myeloma	None		
Lymphoma		< 1	< 1

strate a resembling frequency such as those of Bogumill et al. (6 of 129) [6] or Glicenstein (9 of 471) [1]. The majority of bone tumors that affect the hand are benign lesions. Campanacci and Laus, in a series of 469 cases, reported only ten malignant tumors including six metastases [7]. Murray et al. in 44 primary bone tumors of the wrist reported 38 (86%) benign lesions and 6 (14%) malignant [3]. The most frequent benign bone tumor is enchondroma, whereas the commonest malignant lesion is chondrosarcoma [4].

As a general rule, clinical findings and standard radiography allow an accurate diagnosis of the majority of bone tumors located in the hand or wrist. Ultrasound has no value in assessing bone lesions. Computed tomography is the best modality for careful assessment of bone destruction, whereas MRI can evaluate bone marrow involvement, tumor extension in the adjacent soft tissues, and is the modality of choice in its staging. However, when a malignant lesion is clinically suspected, exhaustive pre-surgical evaluation and a diagnostic biopsy are warranted [8]. Due to their superficial location, malignant tumors of the hand can be early diagnosed and treated successfully if their possibility is kept in mind [9] and a variety of tumor-like conditions, such as MFH, fibrous dysplasia, or glomus tumor are excluded.

Benign tumors

Anatomic variants

Accessory bones of the wrist are frequent and may simulate bone tumors. The most common is the Os Styloideum, a small bone located at the dorsal aspect of the wrist between the third metacarpal and the capitate [10]. The ossicle presents clinically as a protuberance (carpal boss) which can cause painful slipping of the extensor tendons and limitation of movements of the wrist. Differential diagnosis include a ganglion, localized osteoarthritis, and subcutaneous calcification. The radiographic appearance of carpal boss is typical, but specific views must be obtained to detect it. In doubtful cases tomography or high-resolution CT can show the ossicle in better detail. Bone scintigraphy can show focal increase of tracer uptake [10].

Bone islands

Bone islands are well-circumscribed, cortical bone lesions located within trabecular bone. Controversy is still present about their origin. Different hypotheses consider these benign conditions as hamartomas, pseudotumors, or conditions related to altered development of enchondral ossification [11]. They are usually clinically silent and discovered by chance at radiographs obtained for other reasons. Standard radiographs shows ovoid, homogeneous compact bone lesions which can rarely increase in size. A characteristic of bone islands, which has diagnostic relevance since it allows differentiation from sclerotic metastases, is the presence of spiculated borders which blend in the surrounding cancellous trabeculae (Fig. 1). A CT scan can confirm the radiographic findings, but generally no further assessment is required. Although in most cases bone scan is unremarkable, increased uptake of the tracer is observed, particularly in larger lesions. In these cases the peculiar radiographic appearance can differentiate bone islands from other sclerosing lesions such as osteoid osteoma, osteosarcoma, or a solitary sclerotic metastasis [11].

Osteoid osteoma and osteoblastoma

Osteoid osteoma and osteoblastoma are benign osteoblastic tumors that mainly affect the phalanges and metacarpals (Table 1). Osteoid osteoma is observed chiefly in young males. The typical radiographic appearance is that of a small (< 1 cm in size), radiolucent lesion, surrounded by an area of bone sclerosis which accounts for the local increase uptake at bone scan. In cases in which extensive bone sclerosis prevents the

Fig. 1 A 26-year-old man. Bone island of the scaphoid. Oblique pain film of the wrist. An island of compact and homogeneous bone with spicules *(arrow)* is evident in the middle third of the scaphoid

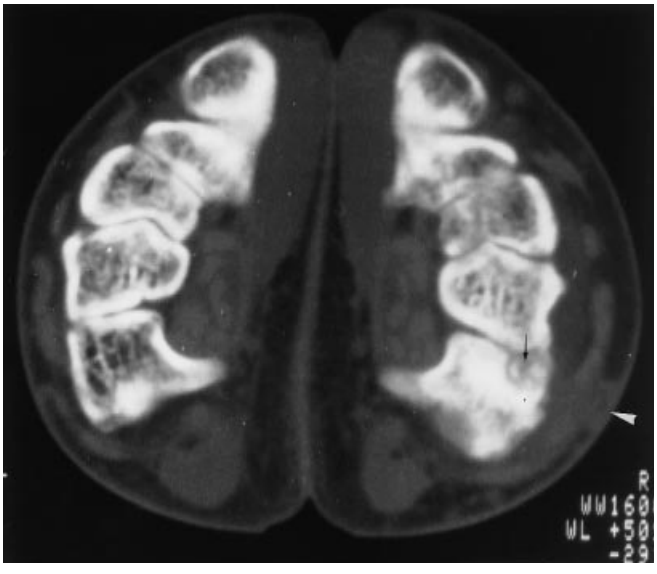

Fig. 2 A 20-year-old man. Osteoid osteoma of the hamate bone. Computed tomography: axial images of both wrists show a small nidus *(arrow)* as a well-marginated lytic lesion surrounded by sclerosis located in the left hamate. Localized synovitis and edema of subcutaneous tissues are also evident *(arrowhead)*

Fig. 3 A 25-year-old woman. Enchondroma of the phalanx. Plain film: anteroposterior view of the fourth finger shows a well-circumscribed osteolytic lesion located in the proximal phalanx. Note thinning of the cortex. A fracture line is evident *(arrow)*

demonstration of the nidus at standard radiographs, CT can show it as a hypodense image surrounded by the reactive sclerotic bone (Fig. 2). Due to high-definition and high-quality multiplanar reconstructions, which allow accurate assessment of nidus location, CT with small collimation (1 mm) is currently the modality of choice in the evaluation of osteoid osteoma. Although it can show the edema of adjacent soft tissues, MRI more carefully displays it as an increased signal area in T2-weighted and short tau inversion recovery (STIR) images [12]. The perilesional edema must be differentiated from local infection [12].

Larger size of the nidus (diameter > 2 cm) is the most important radiological criterion in differentiating osteoblastoma from osteoid osteoma, although higher radiolucency and heterogeneity, as well as more internal calcifications, are also useful findings [8].

Chondral tumors

The most frequent chondral tumor of the hand is the enchondroma. Forty percent of all enchondroma of the body are located in the phalanges, and 10% in the metacarpals, whereas carpal bone location is uncommon. Typically they present with a pathological fracture

Fig. 4 a–d A 55-year-old woman. Enchondroma of the second phalanx of the fourth finger (vs malignant tumor). Magnetic resonance imaging of coronal plane: The lesion *(arrow)* **a** is hypointense on T1-weighted spin echo (SE) and **b** shows heterogeneous enhancement after i. v. injection of gadolinium. **c** Magnetic resonance imaging sagittal plane after i. v. injection of gadolinium: Despite the cortical thinning seen on coronal plane, there is no soft tissue invasion. **d** Plain film 1 year later: The enchondroma, histologically proved, has been treated by curettage and bone graft *(arrows)*; no sign of recurrence

of a short tubular bone (Fig. 3) [8]. More rarely they are diagnosed because of a slowly enlarging mass. Plain radiographs show enchondroma as diaphyso-metaphyseal radiolucent intramedullary lesions containing thin trabeculae and tiny, punctuate, scattered calcifications of the cartilage matrix. Cortical thinning with subsequent expansion of the affected bone are common. Gradient-echo MR images show an hyperintense lesion with scattered hypointense foci related to matrix calcifications. Tiny calcifications, which are readily evident at radiographs, can be overlooked at MRI if only spin-echo sequences are performed due to an insufficient contrast of signals. A possible indication of MRI in the assessment of enchondroma is the evaluation of the extension of tumor in the cases in which malignant transformation is suspected (Fig. 4). Maffucci's syndrome is a

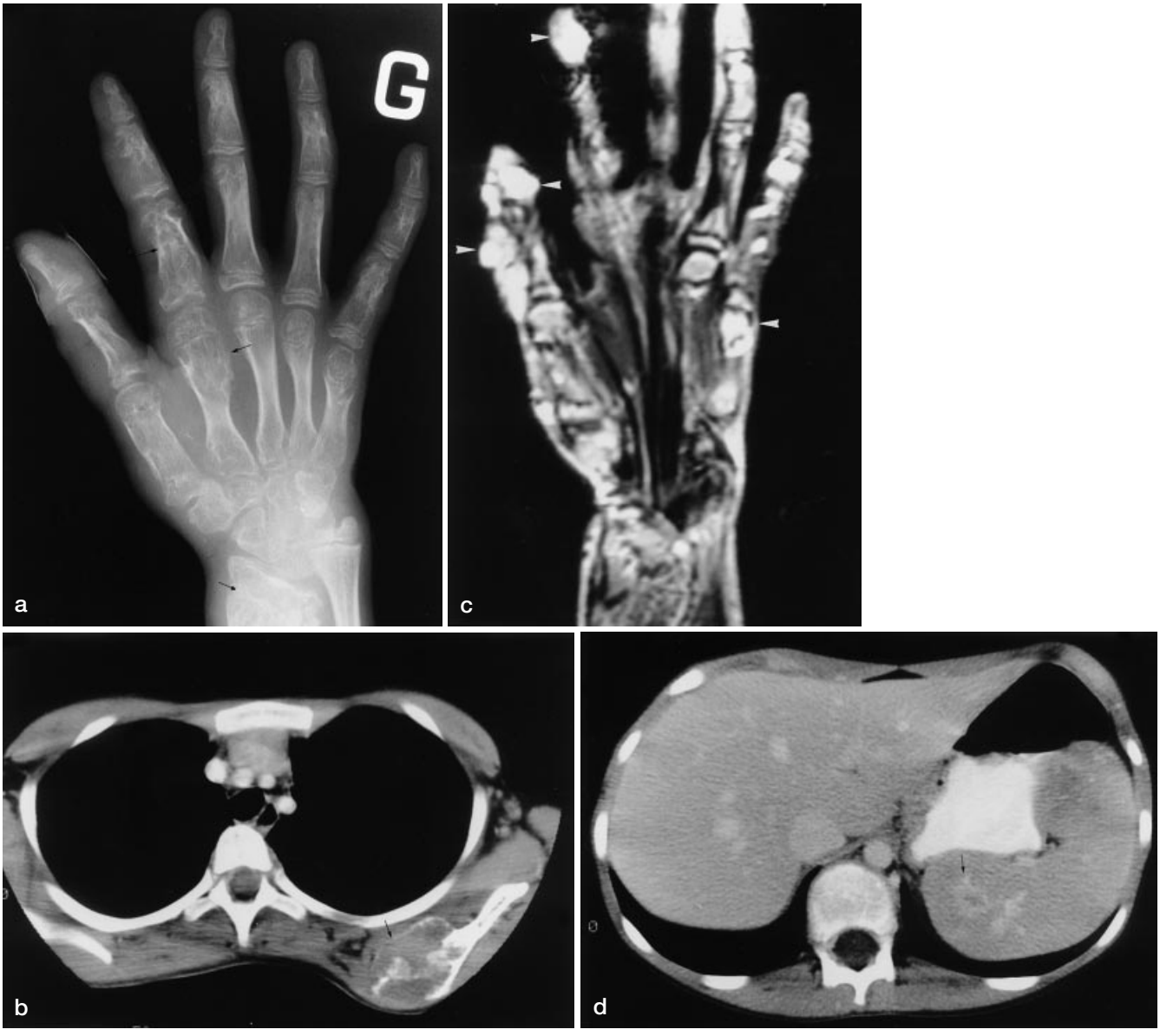

Fig. 5a–d A 12-year-old girl with Maffucci's syndrome. **a** Plain film: multiple enchondromas of the left hand and wrist located mainly in the metaphyses *(arrows)*. **b** Thoracic CT: a large enchondroma destroying the left scapula *(arrow)*. **c** Magnetic resonance imaging of the left hand, in the frontal plane T2-weighted SE: multiple hyperintense nodules *(arrowheads)* corresponding to hemangiomas. **d** Abdominal CT after i.v. injection of iodine contrast: a large hemangioma of the spleen *(arrow)*

congenital dysplasia in which multiple chondromas are associated with soft tissue hemangiomas (Fig. 5).

Chondroblastoma of the hand is extremely rare. Clinical and some imaging findings are similar to those of enchondroma, although chondroblastoma affects more commonly the epiphysis rather then the diaphysis. Chondroblastoma may present a large area of bone marrow and soft tissue edema which is very well depicted on MRI examination. Local recurrence after surgical removal and malignant degeneration can occur.

Osteochondroma of the hand is almost exclusively observed in patients affected by multiple exostosis. Solitary exostosis is extremely rare.

Giant cell tumor

Giant cell tumor, usually observed in young patients (20–40 years), originates in the epiphysis and can expand into the metaphysis and diaphysis. The tumor mainly involves the phalanges and metacarpals and the

Fig. 6 A 37-year-old woman. Giant cells tumor of the radius. Plain film: asymmetric osteolytic lesion of the distal meta-epiphysis of the radius with local expansion of the ulnar aspect and cortex destruction *(arrows)*

distal epiphysis of the radius (Fig. 6). Local aggressive behavior explains the high rate of recurrences after surgical excision [8, 13]. On plain films they appear as a pure lytic lesion with small expansion of the affected bone. Both CT and MRI add little to diagnosis. Their main indication is the assessment of cortical erosion and evaluation of perilesional soft tissues.

Aneurysmal bone cyst

Fuhr and Herndon, in a series of 516 aneurysmal bone cysts, found 17 lesions involving the hand [14]. These lesions can be primary or secondary to other tumors such as chondroblastoma. The most common locations are the phalanges and metacarpal followed by the carpal bones. Standard radiographs show aneurysmal bone cyst as lytic enlarging lesions which often cause a blow-up of the involved bone. Cortical fractures with subsequent periosteal reaction can be demonstrated as well. Although not specific, a fluid–fluid level, which can be detected by CT and MRI, is suggestive of the diagnosis [15]. The high rate of local recurrences after surgical curettage are related mainly to local aggressive behavior.

Intraosseous ganglion

Intraosseous ganglia are common findings at standard radiographs of the wrist and hand. They typically appear as small, well-circumscribed, oval lytic lesions bordered by a sclerotic rim (Fig. 7a). Internal mucoid content presents at MRI as low–intermediate signal on T1- and high signal on T2-weighted images (Fig. 7b, c) [16]. Pathogenesis of intraosseous ganglia is still debated, although a mechanism similar to subchondral cysts observed in rheumatoid arthritis and osteoarthritis is likely.

Malignant tumors

Although uncommon, metastases of the hand are more frequent than primary bone tumors. Of 102 cases reported by Uriburu, the primitive tumor was localized in the lung in 50% and in the breast in 16% (cited in [4]). Phalanges are more commonly involved than metacarpal and wrist. Radiographically, metastases appear as aspecific lytic aggressive lesions which can be misdiagnosed as infection, particularly in older patients, if the primitive tumor is not known [17].

Malignant bone tumors of the wrist and hand are exceptionally rare. Plain films and MRI are the best imaging modalities to estimate local tumor extension and relation with surrounding structures that are the mainstays of operative planning.

Osteogenic sarcoma, a rare tumor with a peak incidence between 10 and 20 years, has a better prognosis when it affects the hand [8]. Magnetic resonance imaging effectively shows the involvement of the soft tissues, which usually is associated with bone destruction and periosteal reaction readily evident at radiographs. Parosteal sarcoma differs from osteogenic sarcoma because of its localization at bone surface, slow grow, late metastases, and better prognosis [8]. Plain radiographs show a lobulated osseous mass connected with the bone surface by a broad stalk. Computed tomography can demonstrate in better detail the stalk, whereas MRI is useful in assessing soft tissues involvement and intramedullary extension.

In the series of Dahlin and Salvador, only 10 of 320 chondrosarcomas were localized in the hand [18]. The distribution of chondrosarcomas of the hand reflects that of chondroma and suggests a likely association be-

Fig. 7 **a** A 32-year-old woman. Intraosseous ganglion cyst. Computed tomography: axial image of the wrist shows a well-delimited lytic lesion surrounded by sclerotic rim located in the scaphoid *(arrow)*. **b, c** A 30-year-old female with intraosseous ganglion cyst. Magnetic resonance imaging: Coronal images show a large intraosseous ganglion cyst located in the radial aspect of the lunate bone. The content of the cyst is hypointense on **b** T1-weighted SE and hyperintense on c fat-saturated T2-weighted images. The cortex is partially destroyed *(arrows)*

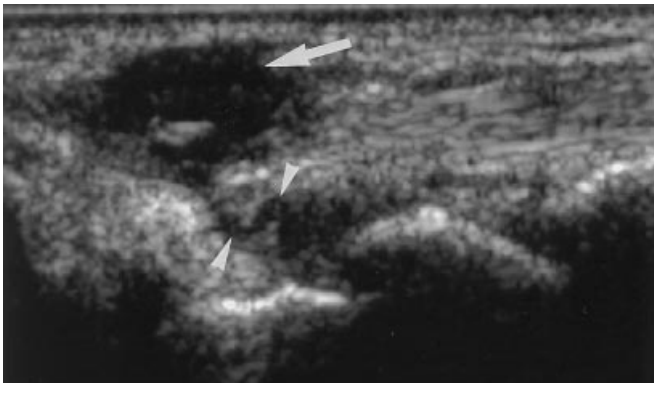

Fig. 8 A 27-year-old woman with dorsal ganglion of the wrist. Ultrasound, sagittal plane: The lesion *(arrow)* appears as a hypoechoic mass located in the subcutaneous tissue. A tortuous pedicle connecting the ganglion to the joint is evident *(arrowheads)*

tween the two conditions. Radiographic findings include a bone lytic lesion with possible matrix calcifications, and cortical destruction with periosteal reaction. Soft tissue involvement, the hallmark of the differential diagnosis vs chondroma, can be accurately estimated by MRI.

Ewing's sarcoma frequently affects young men [19]. Metacarpals are involved in less than 1 % of cases. Lesions that involve the carpal bones have never been described. Radial and ulnar involvement is relatively more frequent, respectively, 2 and 1 % [4]. Ewing's sarcomas can show multicentric medullary foci. Radiographs show bone destruction and periosteal reaction which, if lamellar and thin, is not specific of the condition. Juxtacortical soft tissue involvement is present in approximately 89 % of cases and can be detected easily by MRI [19].

Soft tissue tumors

In a review of 4235 cases of hand tumors from the six larger series (1960–1988) Leclercq and Glicenstein found 70 % of soft tissues lesions [20]. Plain radiographs have a limited diagnostic role in this field, whereas MRI [21, 22] and US [23] are very effective.

Benign tumors

Ganglia

Wrist ganglia, which account for 59 % of soft tissue tumors of the hand, are painless, rounded masses, filled by mucoid fluid and lined by a fibrous wall, located near tendons or joints capsule [20, 24]. The most frequent site is the dorsal aspect of wrist followed by the palmar aspect and the base of fingers [24, 25]. Ganglia can communicate with the adjacent joint cavity, by means of a pedicle which acts as a one-way valve and allows synovial fluid to move from the joint to the cyst. In cases in which no connection with the joint space could be found, ganglia were believed to originate from mucoid degeneration of the periarticular connective tissue [24]. Ultrasound shows ganglia as hypo-anechoic, fluid-filled, expansible periarticular lesions which present distinct borders (Fig. 8) [23, 25]. The wall can be assessed only in chronic lesions in which hyperechoic wall and internal septations are found. Color Doppler shows no internal

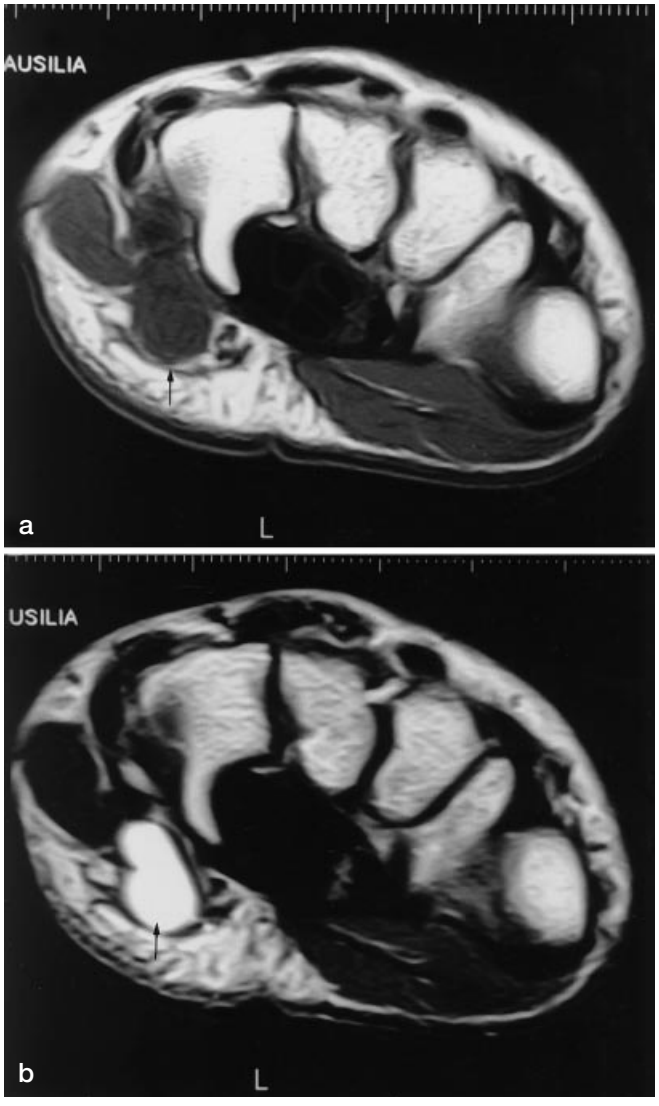

Fig. 9 a, b A 32-year-old woman with ganglion cyst of Guyon's canal. Magnetic resonance imaging axial images obtained at the level of the hook of the hamate bone. A well-demarcated and homogeneous soft tissue mass *(arrows)* **a** with an intermediate signal on T1-weighted SE and **b** highly hyperintense on T2-weighted SE is evident. The lesion is located medially to the hook of the hamate bone, inside the Guyon's canal

flow signal. Smaller ganglia, clinically undetectable, can be diagnosed by US. Magnetic resonance imaging shows a homogeneous cystic lesion iso-intense with muscle on T1-weighted images and hyperintense on T2-weighted images (Fig. 9) [22]. Both techniques readily show the relation of ganglia with the surrounding tendons, nerves, and vessels, and are helpful in the preoperative planning.

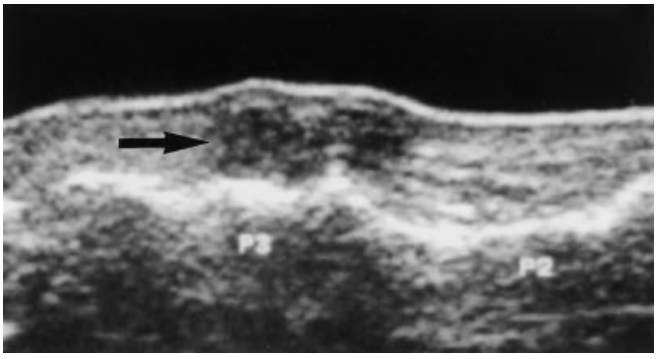

Fig. 10 A 41-year-old woman. Giant cell tumor of tendon sheath. Ultrasound in sagittal plane of the fourth finger: a well-demarcated hypoechoic soft tissue tumor *(arrow)*, located at the palmar aspect of the distal interphalangeal joint. *P2* middle phalanx; *P3* distal phalanx

Giant cell tumor of tendon sheath

Giant cell tumor of tendon sheath (localized villonodular tenosynovitis) is the second most frequent (12%) expansible soft tissue lesion of hand [20]. Characteristic pathological findings include a loose connective tissue in which are found multinucleated giant cells with intracytoplasmic fat and hemosiderin inclusions. Plain films are usually normal or show a soft tissue mass. Bone scalloping due to pressure erosion of the mass on the bone cortex and, less commonly, calcified deposits within the mass, are demonstrated [26]. Ultrasound shows a solid hypoechoic mass which rarely contains internal flow signal at Color Doppler (Fig. 10). Hemosiderin content explains the decreased signal intensity on both T1- and T2-weighted MRI images [27], although other lesions, such as fibroma of the tendon sheath, can show similar findings. The low signal of T2-weighted images is useful because it is rarely encountered in other soft tissue tumors of the hand. Sometimes intralesional heterogeny with a low-signal rim is observed. Usually enhancement of the signal is observed after i.v. injection of gadolinium (Fig. 11).

Lipoma

The incidence of lipoma of the hand is nearly 1%. Clinically they do not differ from lipoma encountered in other locations. They present as soft masses which eventually can be symptomatic due to nerve compression. Computed tomography typically depicts lipoma as well-defined homogeneous lesions of low density (–70 to 100 HU). Magnetic resonance imaging shows a high signal on both T1- and T2-weighted studies and can accurately depict the extension of the lesion. Moreover, T1-weighted MR images obtained

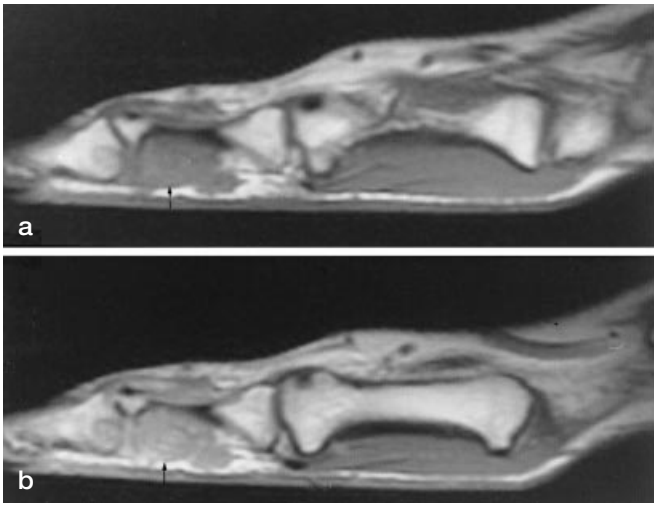

Fig. 11 a, b A 29-year-old woman. Giant cell tumor of tendon sheath. Magnetic resonance imaging in sagittal plane of the first finger: a homogeneous, well-demarcated soft tissue tumor *(arrows)*, with an intermediate signal on **a** T1-weighted SE and **b** enhancement of the signal after i. v. injection of gadolinium

with spectroscopic fat saturation is characteristic of lipoma.

Fibrous tumor

Nerve fibrolipoma (fibrolipomatous hamartoma) is a slow-growing, rare tumor that affects young adults [22]. The most common site is the median nerve. Clinically, patients present a soft tissue mass of the volar aspect of the wrist and evidence of median nerve compression. Ultrasound findings include an irregular, enlarged median nerve. Magnetic resonance imaging shows serpiginous structures with low signal on T1- and T2-weighted images corresponding to the fibrous component embedded in the adipose tissue which have high signal on both sequences [22]. On axial T1-weighted images a characteristic "cable-like" appearance of the tumor is present [28].

Nodular fasciitis and desmoid tumor of the hand are exceptions. Both lesions show local aggressiveness and can be hardly differentiated from sarcomas [20].

Muscle tumors and pseudotumors

Leiomyoma of the hand is relatively frequent compared with involvement of other sites [20]. It appears as small nodules located in the muscles and is treated by surgical excision. Accessory muscles can mimic leiomyoma. The most common accessory muscles of the hand are the accessory flexor digitorum superficialis and extensor

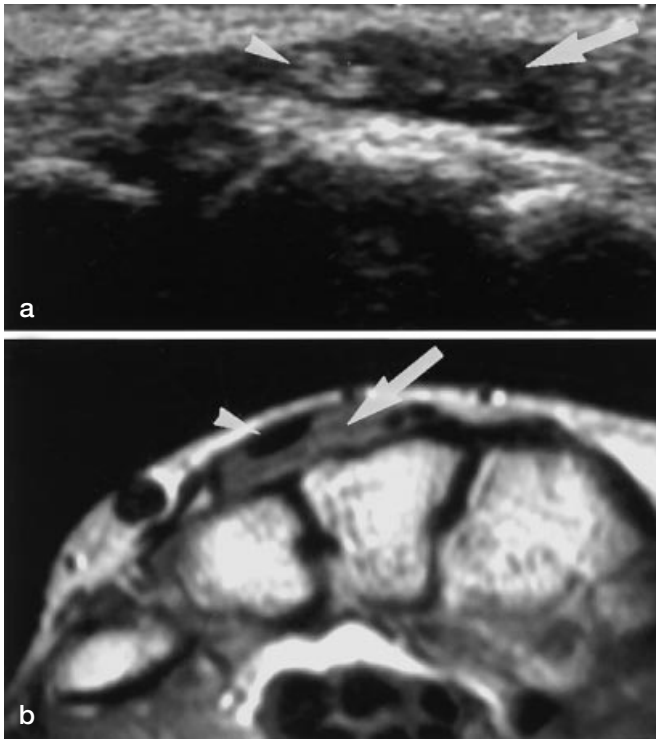

Fig. 12 a, b A 56-year-old man. Accessory muscle: extensor indicis proprius. **a** Ultrasound axial sonogram of the posterior aspect of the wrist: a hypoechoic lesion *(arrow)* with sharp borders located adjacent to the extensor tendon *(arrowheads)*. **b** T1-weighted SE axial MRI image obtained at the same level: a well-demarcated soft tissue tumor *(arrows)*, homogeneous, with an intermediate signal on T1-weighted SE located close to the extensor tendons *(arrowheads)*

indicis proprius. Magnetic resonance imaging shows accessory muscles as elongated masses with distinct margins which present the same signal of normal muscles in all sequences [22]. Ultrasound shows a mass which presents the same echotexture of normal muscle (Fig. 12). Variation of size during active muscle contraction can be demonstrated.

Myositis ossificans circumscripta is readily demonstrated at radiographs. Magnetic resonance imaging can depict it at an early stage, when calcifications are not evident, as a heterogeneous expansive lesion of soft tissue which can be misdiagnosed as a sarcoma [29].

Hemangiomas

Hemangiomas affect more commonly soft tissues than bone. Whereas skin and subcutaneous lesions are readily diagnosed at physical examination, hemangiomas affecting the muscle or synovium require an imaging modalities for proper evaluation [30]. Plain radiographs can show rounded regular calcifications in-

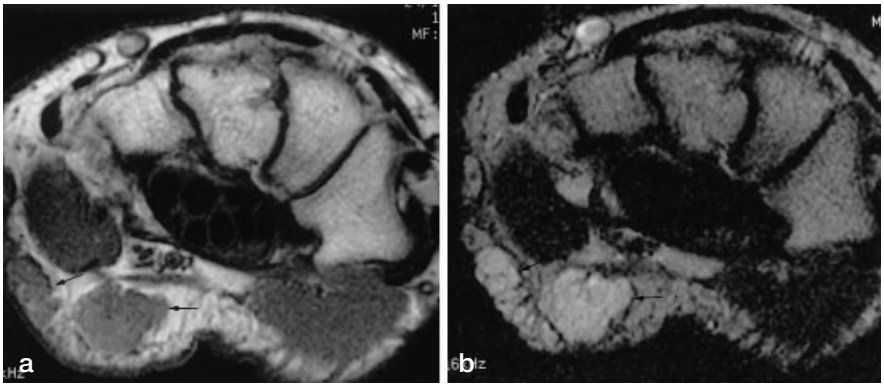

Fig. 13a, b A 43-year-old man. Tuberous angioma of the subcutaneous area. Magnetic resonance imaging axial plane: a lobulated soft tissue mass *(arrows)* with an intermediate signal on **a** T1-weighted SE and moderately hyperintense on **b** T2-weighted SE

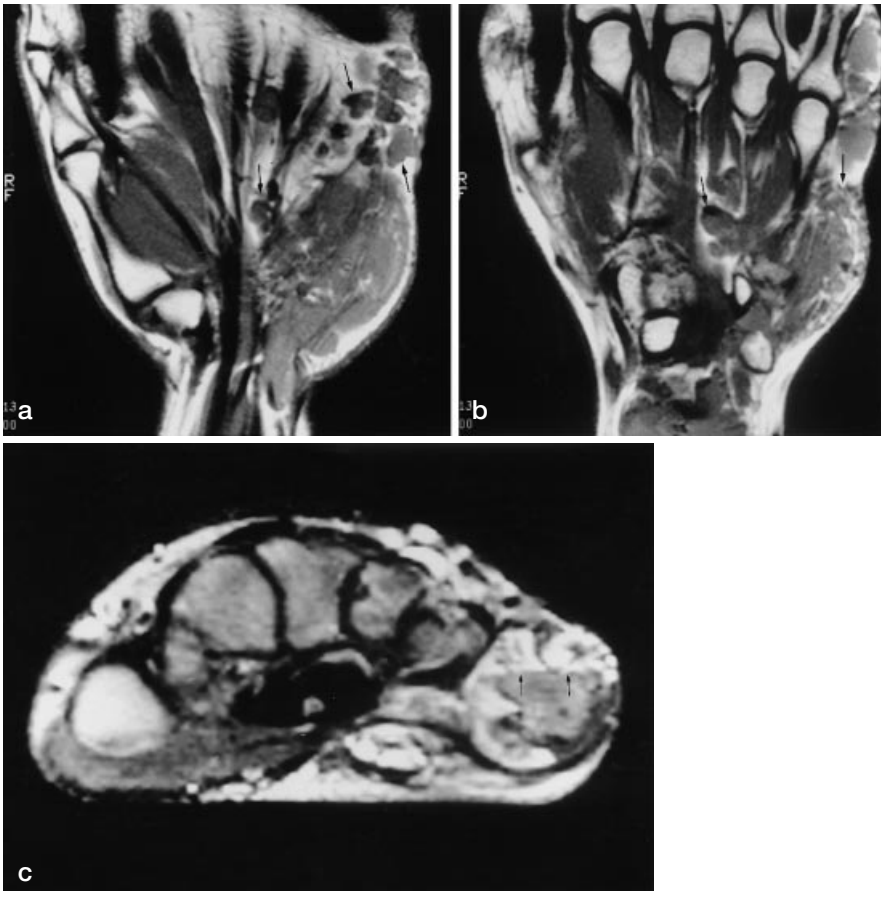

Fig. 14a–c A 17-year-old woman with a large hemangioma of the hand. **a, b** Magnetic resonance imaging frontal plane T1-weighted SE: multiple soft tissue nodules *(arrows)* located into the subcutaneous fat as well as inside the muscles with intermediate signal. **c** Magnetic resonance imaging in axial plane, T2-weighted SE: In the largest lesions fluid–fluid level is visible *(arrows)*

side the mass which correspond to phleboliths contained in the low-flow vessels. Computed tomography shows a mass with contrast enhancement. Angiography depicts the new vascularization but is rarely obtained in small lesions affecting the extremities. Ultrasound and color Doppler readily show the vascular origin of the mass. Magnetic resonance imaging shows intramuscular hemangiomas as masses with aspecific low signal intensity on T1-weighted images and high signal intensity on T2-weighted images (Figs. 13, 14). Nelson et al. reported the usefulness of T2-weighted images obtained with TR of 2000 and a long TE (150 ms), since with such parameters few other lesions present a high signal [31]. Both MRI and US are useful in the assessment of intramuscular hemangiomas. Magnetic resonance imaging is an excellent modality to evaluate the size, contours, and relations with surrounding structures, whereas US confirms the vascular nature. Cavernous hemangiomas can

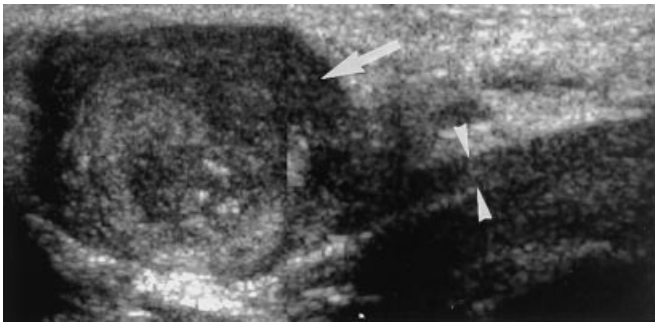

Fig. 15 A 41-year-old man. Schwannoma of the median nerve. Ultrasound double-split image obtained in the sagittal plane: a well-demarcated, hypoechoic mass *(arrow)* with irregular internal echotexture. The lesion appears connected to the median nerve *(arrowheads)*

present at MRI and CT internal fluid levels which, although not pathognomonic, are useful diagnostic findings [32].

Nerve tumors

The two benign nerve tumors, neurofibromas and schwannomas, rarely affect the wrist and hand. Solitary neurofibromas are rare. Multiple neurofibromas are found in Recklingausen's disease. Neurofibromas originate from the fibrous tissue of the epyneurium and grow among the nerve fascicles. This explains why these tumors present hill-defined borders and are difficult to excise [6]. Schwannomas are more clearly delimited since they derive from peripheral Schwann cells. Ultrasound shows nerve tumors as fusiform hypoechoic masses with well-defined margins. A presumptive diagnosis of nerve tumor can reliably be made with US only if the mass is connected to a nerve bundle (Fig. 15). At

Fig. 17 A 38-year-old woman with rhabdomyosarcoma of the hand. Magnetic resonance imaging of frontal plane on T1-weighted SE after i.v. injection of gadolinium. The tumor located between the flexor tendons and muscles of the hypotenar eminence appears heterogeneous with central areas of low signal intensity *(arrowheads)* and enhancement at the periphery *(arrows)*

MRI nerve tumors appear isointense or slightly hypointense to muscle on T1-weighted images and hyperintense on T2-weighted images. Usually a homogenous internal pattern is evident, but a diagnosis of benign lesion is sometimes difficult [22].

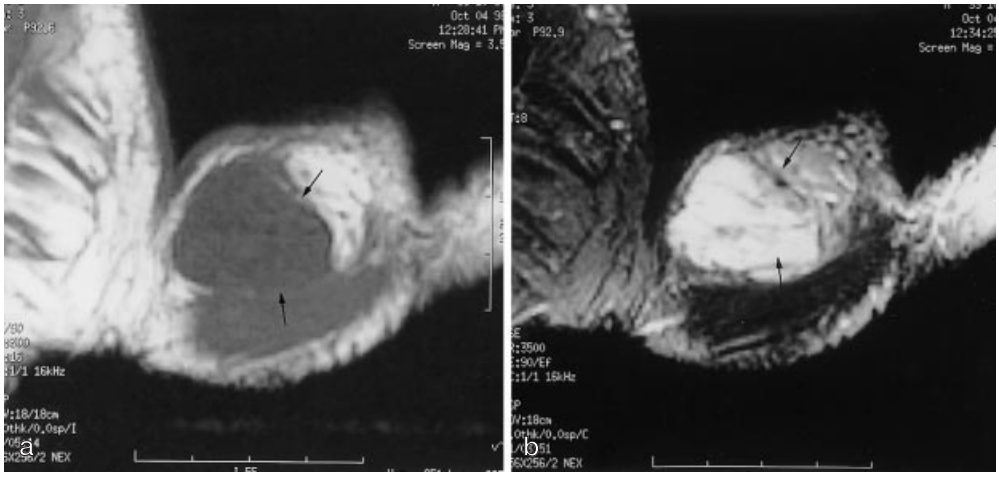

Fig. 16 a, b A 33-year-old man with a soft tissue primary neuroectodermic tumor. Magnetic resonance imaging in coronal plane: a soft tissue mass *(arrows)* homogeneous, well demarcated, **a** with an intermediate signal on T1-weighted SE and **b** highly hyperintense, in relation to the adjacent muscle, on fat-saturated T2-weighted images

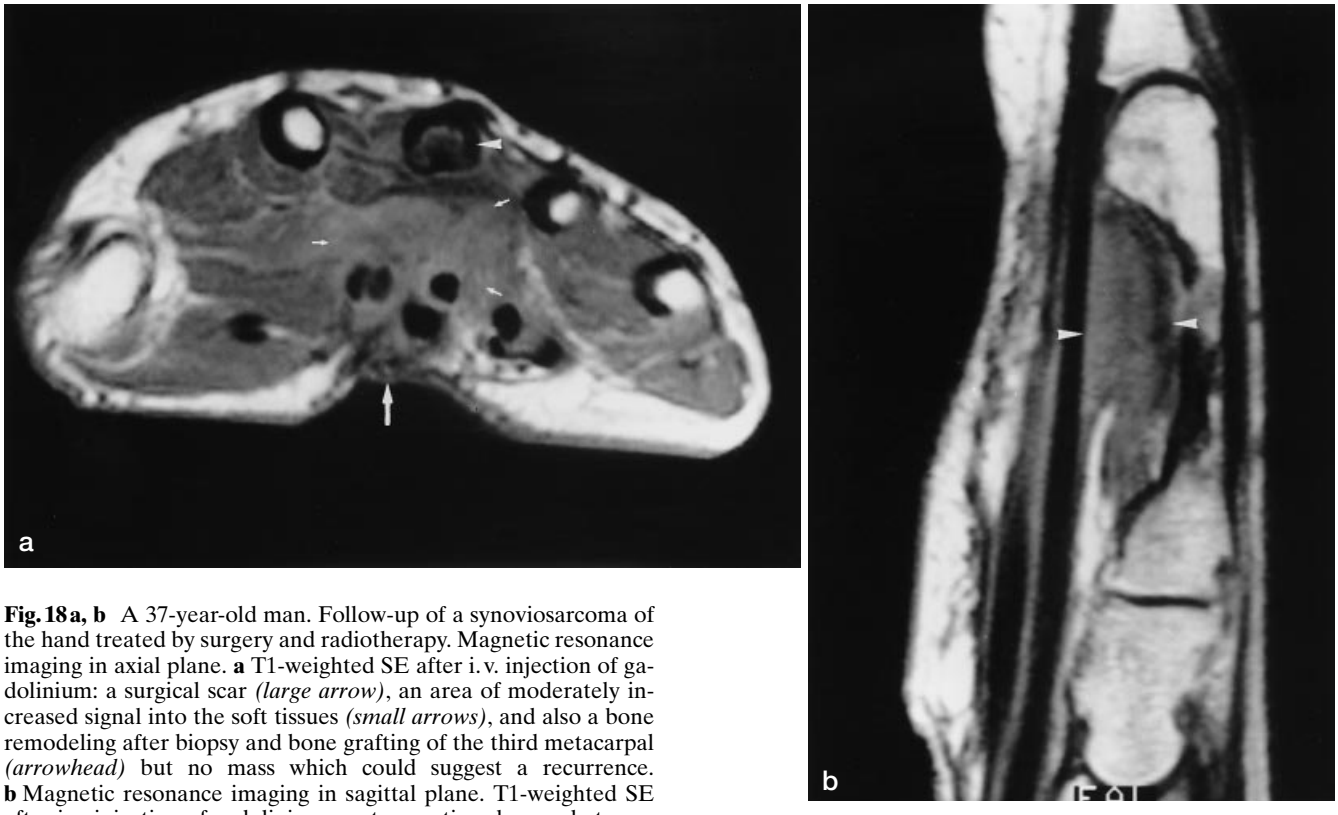

Fig. 18 a, b A 37-year-old man. Follow-up of a synoviosarcoma of the hand treated by surgery and radiotherapy. Magnetic resonance imaging in axial plane. **a** T1-weighted SE after i.v. injection of gadolinium: a surgical scar *(large arrow)*, an area of moderately increased signal into the soft tissues *(small arrows)*, and also a bone remodeling after biopsy and bone grafting of the third metacarpal *(arrowhead)* but no mass which could suggest a recurrence. **b** Magnetic resonance imaging in sagittal plane. T1-weighted SE after i.v. injection of gadolinium: post-operative changes between the flexor tendons and the third metacarpal *(arrowheads)*

Malignant tumors

Soft tissue sarcomas of the hand are very rare. Some sarcomas, such as synoviosarcomas (10% of all soft tissue tumors), are most frequent, particularly the subset epitheloid sarcoma which affects in a high percentage of cases (43%) the hand [33]. The imaging of sarcoma is based on standard radiographs which show matrix calcifications and bone erosions, and MRI allows a more valuable assessment of the tumor extension (Fig. 16). Often it is difficult to differentiate between benign and malignant lesions at MRI. Internal irregularity, often not readily apparent on T1-weighted images and more evident on T2-weighted images and T1-weighted post-gadolinium images, is the most specific criterion in the diagnosis of a malignant tumor (Fig. 17); however, it must be stressed that there are no definite MRI criteria between benign and malignant lesions since malignant tumor can be homogeneous and regular. In all patients with a possible malignat tumor, based on the clinical features, a biopsy is recommended regardless of the imaging findings. Although in the great majority of cases MRI does not allow a definite histological diagnosis, it is the best imaging technique for the detection of recurrence of soft tissue sarcoma. Demonstration of a local mass is the best criterion of local recurrence. The lesion usually presents low signal on T1-weighted images, contrast enhancement after gadolinium injection, and high signal on T2-weighted images. The T2-weighted spin-echo fat-saturated sequence is most useful in the detection of local recurrences. Other findings, such as scars, fluid collection, or fibrous lesions, are related to the previous surgery (Fig. 18).

References

1. Glicenstein J (1995) Les tumeurs. Introduction. In: Tubiana R (ed) Chirurgie de la main. Masson, Paris, pp 730–731
2. Dahlin DC (1995) Bone tumors. General aspects and data on 6221 cases, 3rd edn. Thomas, Springfield, Illinois
3. Murray PM, Berger RA, Inwards CY (1999) Primary neoplasms of the carpal bones. J Hand Surg [Am] 24: 1008–1013
4. Wilner D (1982) Radiology of bone tumors and allied disorders. Saunders, Philadelphia
5. Haber MH, Alter AH, Wheelock MC (1965) Tumors of the hand. Surg Gynecol Obstet 121: 1073–1080
6. Bogumill GP, Sullivan DJ, Baker GI (1975)Tumors of the hand. Clin Orthop 108: 214–222

7. Campanacci M, Laus M (1979) Tumors of bone and soft tissues of the hand (a review of 840 cases). Riv Chir Mano 16: 359–363
8. McCullough CJ, Thomine J-M (1995) Tumeurs osseuses de la main. In: Tubiana R (ed) Chirurgie de la main. Masson, Paris, pp 732–752
9. Bogumill GP (1988) Tumors of the wrist. In: Lichtmann DM (ed) The wrist and its disorders. Saunders, Philadelphia, pp 373–384
10. Conway WF, Destouet JM, Gilula LA, Bellinghausen HW, Weeks PM (1985) The carpal boss: an overview of radiographic evaluation. Radiology 156: 29–31
11. Greenspan A (1995) Bone island (enostosis): current concept. A review. Skeletal Radiol 24: 111–115
12. Biebuyck J-C, Katz LD, McCauley T (1993) Soft tissue edema in osteoid osteoma. Skeletal Radiol 22: 37–41
13. Dahlin DC, Cupps RE, Johnson NW (1970) Giant-cell tumor: a study of 195 cases. Cancer 25: 1061–1066
14. Fuhr SE, Herndon JH (1979) Aneurysmal bone cyst involving the hand. A review and report of two cases. J Hand Surg 4: 152–159
15. Sullivan RJ, Meyer JS, Dormans JP, Davidson RS (1999) Diagnosing aneurysmal and unicameral bone cysts with magnetic resonance imaging. Clin Orthop 366: 186–190
16. Tanaka H, Araki Y, Yamamoto H, Yamamoto T, Tsukaguchi Y (1995) Intraosseous ganglion. Skeletal Radiol 24: 155–177
17. Abrahams TG (1995) Occult malignancy presenting as metastatic disease to the hand and wrist. Skeletal Radiol 24: 135–137
18. Dahlin DC, Salvador AH (1974) Chondrosarcoma of the bones of the hands and feet. Cancer 34: 755–760
19. Coombs RJ, Zeiss J, Paley KJ, Kini J (1993) Case report 802. Ewing's tumor od the proximal phalanx of the third finger with radiographic progression documented over a 6-year-period. Skeletal Radiol 22: 460–463
20. Leclercq C, Glicenstein J (1995) Tumeurs des parties molles de la main. In: Tubiana R (ed) Chirurgie de la main. Masson, Paris, pp 753–772
21. Capelastegui A, Astigarraga E, Fernandez-Canton G, Saralegui I, Larena JA, MerinoA(1999) Masses and pseudomasses of the hand and wrist: MR findings in 134 cases. Skeletal Radiol 28: 498–507
22. Miller TT, Potter HG, McCormack RR (1994) Benign soft tissue masses of the wrist and hand: MRI appearances. Skeletal Radiol 23: 327–332
23. Bianchi S, Abdelwahab IF, Zwass A, Giacomello P (1994) Ultrasonographic evaluation of wrist ganglia. Skeletal Radiol 23: 201–203
24. Razemon JP (1995) Les kystes du poignet. In: Tubiana R (ed) Chirurgie de la main. Masson, Paris, pp 627–633
25. Bianchi S, Abdelwahab IF, Zwass A, Calogera R, Banderali A, Brovero P, Votano P (1993) Sonographic findings in examination of digital ganglia: retrospective study. Clin Radiol 48: 45–47
26. Karasick D, Karasick S (1992) Giant cell tumor of tendon sheath: spectrum of radiologic findings. Skeletal Radiol 21: 219–224
27. De Beuckeleer L, De Schepper A, De Belder F, Van Goethem J, Marques MC, Broeckx J, Verstraete K, Vermaut F (1997) Magnetic resonance imaging of localized giant cell tumour of the tendon sheath (MRI of localized GCTTS). Eur Radiol 7: 198–201
28. Evans HA, Donnelly LF, Johnson ND, Blebea JS, Stern PJ (1997) Fibrolipoma of the median nerve: MRI. Clin Radiol 52: 304
29. Ehara S, Nishida J, Abe M, Mizutani H, Ohba S (1994) Magnetic resonance imaging of pseudomalignant osseous tumor of the hand. Skeletal Radiol 23: 513–516
30. Greenspan A, McCahan JP, Vogelsang P, Szabo RM (1992) Imaging strategies in the evaluation of soft tissue hemangiomas of the extremities: correlation of the findings on plain radiography, angiography, CT, MRI and ultrasonography in 12 histologically proven cases. Skeletal Radiol 21: 11–18
31. Nelson MC, Stull MA, Teitelbaum GP, Paat RH, Lack EE, Bogumill GP, Feedman MT (1990) Magnetic resonance imaging of peripheral soft tissue hemangiomas. Skeletal Radiol 19: 477–483
32. Ehara S, Sone M, Tamakawa Y, Nishida J, Abe M, Hachiya J (1994) Fluid–fluid levels in cavernous hemangioma of soft tissue. Skeletal Radiol 23: 107–109
33. Enzinger FM (1970) Epitheloid sarcoma, a sarcoma simulating a granuloma or a carcinoma. Cancer 26: 1029–1041